Emulating quantum state transfer through a spin-1 chain on a one-dimensional lattice of superconducting qutrits

Joydip Ghosh*
Institute for Quantum Science and Technology, University of Calgary, Calgary, Alberta T2N 1N4, Canada
(Received 13 October 2014; published 10 December 2014)

Spin-1 systems, in comparison to spin-$\frac{1}{2}$ systems, offer a better security for encoding and transferring quantum information, primarily due to their larger Hilbert spaces. Superconducting artificial atoms possess multiple energy levels, thereby being capable of emulating higher-spin systems. Here I consider a one-dimensional lattice of nearest-neighbor-coupled superconducting transmon systems, and devise a scheme to transfer an arbitrary qutrit state (a state encoded in a three-level quantum system) across the chain. I assume adjustable couplings between adjacent transmons, derive an analytic constraint for the control pulse, and show how to satisfy the constraint to achieve a high-fidelity state transfer under current experimental conditions. My protocol thus enables enhanced quantum communication and information processing with promising superconducting qutrits.

DOI: 10.1103/PhysRevA.90.062318 PACS number(s): 03.67.Ac, 85.25.Hv, 03.67.Hk

I. INTRODUCTION

Quantum state transfer (QST) between two quantum systems remains a primitive operation for many protocols in quantum communication, simulation, and information processing. QST along a chain of nearest-neighbor-coupled spin-$\frac{1}{2}$ systems has been extensively studied as a channel for short-distance quantum communication [1–7], and its implementations have been proposed for NMR systems [8–10], trapped Rydberg ions [11], coupled-cavity arrays [12], and superconducting flux qubits [13], with experimental realizations reported so far for NMR systems [14], photonic lattices [15,16], and cold atoms [17,18]. However, with the discovery that quantum information processing becomes more robust on higher-dimensional spin systems [19,20], considerable attention has been paid to the higher-dimensional spin chains. This leads to the emergence of a number of proposals in recent years for possible QST schemes on d-level ($d > 2$) spin chains, specifically on spin-1 chains [21–27].

Superconducting artificial atoms contain more than two energy levels that can be readily manipulated and reliably measured, thereby allowing the possibility of emulating the higher spin systems [28]. In this work, I devise a scheme to emulate a QST along a spin-1 chain on a one-dimensional array of nearest-neighbor-coupled superconducting transmon systems [29]. The transmons are treated as *qutrits* (three-level systems) with the three lowest energy levels mapping to the three possible states of a spin-1 particle. I also assume an adjustable coupling between each pair of adjacent transmons that can be tuned via control electronics, an architecture often referred to as a *gmon* device [30,31]. It should be emphasized in this context that when two transmons are coupled (via an inductive tunable coupler), the coupling strengths in the single- and double-excitation subspaces are unequal requiring two different time scales to transfer quantum states for those two subspaces. These unequal coupling strengths, in fact, preclude a direct generalization from a qubit-to-qubit state transfer to a qutrit-to-qutrit state transfer for superconducting systems, which motivates us to develop a strategy for such a higher-dimensional state transfer across the chain of superconducting qutrits under experimental conditions.

The problem of emulating the QST on the array of coupled transmon qutrits can be described as follows: First, I prepare an arbitrary qutrit state $|\psi\rangle = \alpha|0\rangle + \beta|1\rangle + \gamma|2\rangle$ in the first qutrit (as demonstrated by Neeley *et al.* [28]), and then control the tunable coupling strengths for a specific time-duration such that

$$|\psi\rangle_1 \otimes |0\rangle_2 \otimes |0\rangle_3 \otimes \cdots \otimes |0\rangle_N \longrightarrow |0\rangle_1 \otimes |0\rangle_2 \otimes |0\rangle_3 \otimes \cdots \otimes |\psi\rangle_N, \quad (1)$$

where the subscripts denote the qutrit indices and N is the number of transmons in the array. The transformation shown in Eq. (1) is achieved via successive state transfers between adjacent qutrits, given by

$$|\psi\rangle_j \otimes |0\rangle_{j+1} \longrightarrow |0\rangle_j \otimes |\psi\rangle_{j+1}, \quad \forall\, j \in \{1,2,\ldots,N-1\}. \quad (2)$$

Note that in order to perform the state transfer between adjacent qutrits, it is necessary and sufficient that the operations

$$\begin{aligned} |1\rangle_j \otimes |0\rangle_{j+1} &\longrightarrow |0\rangle_j \otimes |1\rangle_{j+1}, \\ |2\rangle_j \otimes |0\rangle_{j+1} &\longrightarrow |0\rangle_j \otimes |2\rangle_{j+1}, \end{aligned} \quad (3)$$

are performed simultaneously with other states unchanged. Here I show how to achieve such a simultaneous state transfer with superconducting qutrits under current experimental constraints.

The remainder of the paper is organized as follows: I first discuss the state transfer between two coupled qutrits in Sec. II. Next, I describe my QST protocol across the array of coupled qutrits in Sec. III. The effects of intrinsic and decoherence-induced errors are discussed in Sec. IV, and I conclude with possible future directions in Sec. V.

II. QUANTUM STATE TRANSFER BETWEEN TWO QUTRITS

Here I focus on the QST between two coupled superconducting qutrits. First I describe the coupled-qutrit model and then discuss my state-transfer protocol.

*ghoshj@ucalgary.ca

A. Coupled-qutrit model

The Hamiltonian of a system of two superconducting transmon devices coupled via an adjustable inductive coupling (the 'gmon' architecture [30,31]) is given by (from the laboratory frame)

$$H(t) = \sum_{i=1}^{2} \begin{bmatrix} 0 & 0 & 0 \\ 0 & \epsilon_i(t) & 0 \\ 0 & 0 & 2\epsilon_i(t) - \eta_i \end{bmatrix}_{q_i} + g(t) X_1 X_2, \tag{4}$$

where

$$X_k = \begin{bmatrix} 0 & 1 & 0 \\ 1 & 0 & \sqrt{2} \\ 0 & \sqrt{2} & 0 \end{bmatrix}_{q_k}, \tag{5}$$

where k denotes the qutrit index, and the matrix subscripts $q_{1,2}$ denote the matrix representations of the corresponding operators for the first and the second qutrit, respectively. ϵ_i in Eq. (4) denotes the frequency of the ith qutrit that can be tuned with external control electronics. g denotes the adjustable coupling strength between two qutrits that can be varied between 0 and 55 MHz [30]. η_i is the anharmonicity of the ith qutrit, and here we assume $\eta_1 = \eta_2 = \eta$ (= 200 MHz) [32].

To transform the Hamiltonian (4) from a laboratory frame to a rotating frame, we specify a local reference clock for each qutrit (with frequencies ω_1 and ω_2) with a clock Hamiltonian,

$$H_{\rm cl} = \begin{bmatrix} 0 & 0 & 0 \\ 0 & \omega_1 & 0 \\ 0 & 0 & 2\omega_1 \end{bmatrix}_{q_1} + \begin{bmatrix} 0 & 0 & 0 \\ 0 & \omega_2 & 0 \\ 0 & 0 & 2\omega_2 \end{bmatrix}_{q_2}. \tag{6}$$

The unitary operator corresponding to the rotating frame specified by the clock-Hamiltonian (6) is defined as

$$R(t) \equiv e^{i H_{\rm cl} t}. \tag{7}$$

The Hamiltonian from the rotating frame is then given by

$$\begin{aligned} \widetilde{H}(t) &= R^{\dagger}(t) H(t) R(t) - i \dot{R}^{\dagger}(t) R(t) \\ &= \sum_{i=1}^{2} \begin{bmatrix} 0 & 0 & 0 \\ 0 & \Delta_i(t) & 0 \\ 0 & 0 & 2\Delta_i(t) - \eta_i \end{bmatrix}_{q_i} + g(t) V, \end{aligned} \tag{8}$$

where

$$\Delta_{1,2}(t) = \epsilon_{1,2}(t) - \omega_{1,2},$$

$$V = \begin{bmatrix} 0 & A & 0 \\ B & 0 & A\sqrt{2} \\ 0 & B\sqrt{2} & 0 \end{bmatrix}, \quad \text{with}$$

$$A := \begin{bmatrix} 0 & e^{i(\omega_1+\omega_2)} & 0 \\ e^{i(\omega_1-\omega_2)} & 0 & \sqrt{2}e^{i(\omega_1+\omega_2)} \\ 0 & \sqrt{2}e^{i(\omega_1-\omega_2)} & 0 \end{bmatrix},$$

$$B := \begin{bmatrix} 0 & e^{i(\omega_2-\omega_1)} & 0 \\ e^{-i(\omega_1+\omega_2)} & 0 & \sqrt{2}e^{i(\omega_2-\omega_1)} \\ 0 & \sqrt{2}e^{-i(\omega_1+\omega_2)} & 0 \end{bmatrix}. \tag{9}$$

Note that the interaction term V in Eq. (8) contains rapidly oscillating elements rotating with a frequency $\omega_1 + \omega_2$. Assuming $\omega_1 = \omega_2$ (a global clock) and applying the rotating-wave approximation (RWA) to remove these rapidly oscillating terms, for which the Hamiltonian (8) can be expressed as

$$\begin{aligned} \widetilde{H}(t) = &\sum_{i=1}^{2} \begin{bmatrix} 0 & 0 & 0 \\ 0 & \Delta_i(t) & 0 \\ 0 & 0 & 2\Delta_i(t) - \eta_i \end{bmatrix}_{q_i} \\ &+ \frac{g(t)}{2}(X_1 X_2 + Y_1 Y_2), \end{aligned} \tag{10}$$

where

$$Y_k = \begin{bmatrix} 0 & -i & 0 \\ i & 0 & -i\sqrt{2} \\ 0 & i\sqrt{2} & 0 \end{bmatrix}_{q_k}, \ \forall\, k \in \{1,2\}, \tag{11}$$

and X_k is defined in Eq. (5). $\Delta_{1,2}$ are time-dependent frequencies of the qutrits from the rotating frame that can be varied within -2.5 to $+2.5$ GHz using control electronics. Also, it is interesting to note that the transformation from laboratory frame to rotating frame, in fact, changes the interaction part of our Hamiltonian from XX type to XY type under the RWA.

B. Population transfer between two qutrits

Now I describe how to transfer the population from one qutrit to another. To perform the population transfer, it is sufficient to transform $|00\rangle \leftrightarrow |00\rangle$, $|10\rangle \leftrightarrow |01\rangle$, and $|20\rangle \leftrightarrow |02\rangle$ simultaneously. These simultaneous transformations can be achieved by bringing the qutrits in resonance (i.e., $\Delta_1 = \Delta_2$) and then turning the coupling on under certain constraints, which we derive analytically in this section.

First, it is important to note that the $|00\rangle$ state is sufficiently detuned from all other energy levels when the qutrits are in resonance, and therefore remains invariant even if the coupling is turned on. We represent the Hamiltonian (10) in the single-excitation subspace $\{|01\rangle, |10\rangle\}$ (denoted by $\widetilde{H}_1$) and double-excitation subspace $\{|11\rangle, |02\rangle, |20\rangle\}$ (denoted by $\widetilde{H}_2$) as (after energy rescaling and with $\Delta_1 = \Delta_2$)

$$\widetilde{H}_1(t) = \begin{bmatrix} 0 & g \\ g & 0 \end{bmatrix} \quad \text{and}$$

$$\widetilde{H}_2(t) = \begin{bmatrix} \eta & g\sqrt{2} & g\sqrt{2} \\ g\sqrt{2} & 0 & 0 \\ g\sqrt{2} & 0 & 0 \end{bmatrix}, \tag{12}$$

where the time dependence is embedded in g. In the notation of Pauli spin matrices, $\widetilde{H}_1(t) = g(t)\sigma^x$, and therefore, a population transfer in the single-excitation subspace requires

$$\int_0^{t_{\rm QST}} g(t) dt = \frac{m\pi}{2}, \tag{13}$$

where m is an odd number and $t_{\rm QST}$ denotes the time required for the quantum state transfer.

How about a population transfer in the $\{|02\rangle, |20\rangle\}$ subspace? Note that the levels $|02\rangle$ and $|20\rangle$ are not directly coupled, but coupled via $|11\rangle$ state. The instantaneous eigenvalues of $\widetilde{H}_2$ are 0 and $\eta/2 \pm \sqrt{(\eta/2)^2 + (2g)^2}$, when the qutrits are in resonance. We can, therefore, construct an effective coupling

$g_{\rm eff}$ between $|02\rangle$ and $|20\rangle$ states from the level repulsion between these states, which is given by

$$g_{\rm eff} = \left| \frac{\eta}{4} - \sqrt{\left(\frac{\eta}{4}\right)^2 + g^2} \right|. \tag{14}$$

Following the same argument as for single-excitation subspace, we can express the condition for population transfer between $|20\rangle$ and $|02\rangle$ states as

$$\int_0^{t_{\rm QST}} g_{\rm eff}(t)dt = \int_0^{t_{\rm QST}} \left| \frac{\eta}{4} - \sqrt{\left(\frac{\eta}{4}\right)^2 + [g(t)]^2} \right| dt = \frac{l\pi}{2}, \tag{15}$$

where l is an odd number. Since $g \gg g_{\rm eff}$ ($\approx 2g^2/\eta$) (assuming $\eta \gg g$), the population transfer in the single-excitation subspace is faster than that in the double-excitation subspace, which motivates us to assume $l = 1$ and $m > 1$. Now, combining Eqs. (13) and (15), we obtain the condition for population transfer between qutrits as

$$\int_0^{t_{\rm QST}} g(t)dt = m \int_0^{t_{\rm QST}} \left| \frac{\eta}{4} - \sqrt{\left(\frac{\eta}{4}\right)^2 + [g(t)]^2} \right| dt = \frac{m\pi}{2}, \tag{16}$$

where m is an odd number, and I later show that it is possible to constrain g within an experimentally feasible range for $m = 3$.

C. Designing a control pulse for $g(t)$

Now we use Eq. (16) to design a trapezoidal pulse for $g(t)$ with $g(0) = g(t_{\rm QST}) = 0$ [33]. Let $g_{\rm max}$ be the maximum value that $g(t)$ achieves in the intermediate time, which gives

$$\int_0^{t_{\rm QST}} g(t)dt = g_{\rm max}(t_{\rm QST} - 2) = \frac{3\pi}{2}, \tag{17}$$

assuming $m = 3$ and a 2-ns ramp as shown in Fig. 1(a). The 2-ns ramp is consistent with the bandwidth specification of existing superconducting control electronics [30].

Now, we estimate an approximate value for $g_{\rm max}$, assuming that the area traced out by $g(t)$ and $g_{\rm eff}(t)$ during the constant part of the trapezoidal pulse are almost equal, which essentially means that

$$g_{\rm max} = 3 \left| \frac{\eta}{4} - \sqrt{\left(\frac{\eta}{4}\right)^2 + g_{\rm max}^2} \right|. \tag{18}$$

Solving for $g_{\rm max}$ from Eq. (18) and then $t_{\rm QST}$ from Eq. (17), we obtain

$$g_{\rm max} = \frac{3\eta}{16} \quad \text{and} \quad t_{\rm QST} = 2 + \frac{8\pi}{\eta}. \tag{19}$$

For $\eta = 200$ MHz, $g_{\rm max} = 37.5$ MHz and $t_{\rm QST} = 22$ ns.

It is possible to further improve the performance of qutrit-qutrit population transfer by optimizing $g_{\rm max}$ and $t_{\rm QST}$ independently, using the analytical values as initial solutions. Figure 1(a) shows such an optimal trapezoidal pulse for $g(t)$ with $\Delta_1 = \Delta_2$, and $\eta = 200$ MHz. Table I summarizes the analytical estimates and optimal numerical values for $g_{\rm max}$ and $t_{\rm QST}$.

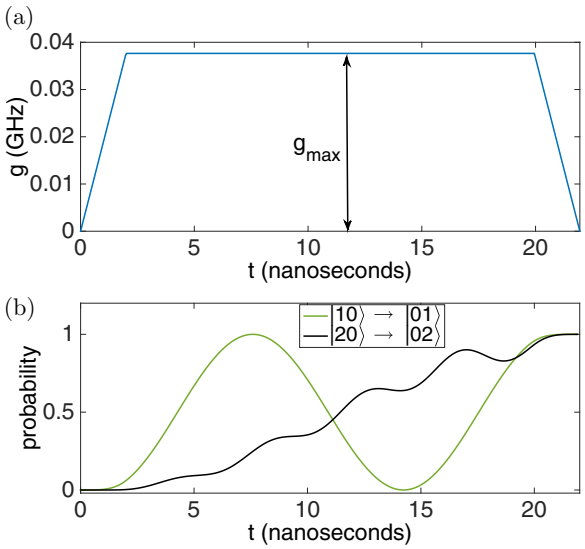

FIG. 1. (Color online) (a) Optimal trapezoidal control pulse for $g(t)$ while two qutrits are in resonance. (b) Probability of population in the $|01\rangle$ and $|02\rangle$ states under the trapezoidal pulse, assuming that the $|10\rangle$ and $|20\rangle$ states are occupied initially.

Figure 1(b) shows the probabilities of population transfer as a function of time for $|10\rangle \rightarrow |01\rangle$ and $|20\rangle \rightarrow |02\rangle$ transitions under the optimal trapezoidal pulse shown in Fig. 1(a). As mentioned earlier, population transfer in the $\{|10\rangle,|01\rangle\}$ subspace is faster than that in the $\{|20\rangle,|02\rangle\}$ subspace, and in my protocol I set a specific value for $g_{\rm max}$ such that these transfers occur simultaneously, coinciding the first peak for the latter with the second peak for the former case. In contrast with the qubit-qubit state transfer, this unusual matching is, in fact, necessary for qutrit-qutrit state transfer, and probably the only choice that satisfies current experimental constraints for superconducting devices. The oscillation observed for the $|20\rangle \rightarrow |02\rangle$ transition in Fig. 1(b) is due to the interference with the $|11\rangle$ state in the double-excitation subspace.

D. Compensating phases

In the population transfer protocol described above, the double-excitation subspace acquires a phase (in the rotating frame), $\varphi = \eta t_{\rm QST}$, with respect to the $\{|00\rangle,|01\rangle,|10\rangle\}$ subspace. My state-transfer protocol, therefore, consists of

TABLE I. Parameters for the control pulse and the corresponding fidelities [defined in Eq. (26)]. Analytical estimates are computed from Eq. (19) and numerical values are obtained via optimization of $g_{\rm max}$ and $t_{\rm QST}$ independently.

Parameters	Values	
	Numerical	Analytical
$g_{\rm max}$ (MHz)	37.7	37.5
$t_{\rm QST}$ (ns)	21.95	22
$\mathcal{F}$ (%)	99.996	99.992

the population transfer plus compensating for the additional phases acquired by any of the basis states. Here I discuss how to compensate for any arbitrary phase acquired by a superconducting qutrit. The Hamiltonian for a single superconducting qutrit in a rotating frame is given by (in the computational basis)

$$\widetilde{H}_{\rm q}(t) = \begin{bmatrix} 0 & 0 & 0 \\ 0 & \Delta(t) & 0 \\ 0 & 0 & 2\Delta(t) - \eta \end{bmatrix}. \tag{20}$$

To perform an arbitrary phase rotation,

$$U_{\rm phase} = \begin{bmatrix} 1 & 0 & 0 \\ 0 & e^{-i\theta} & 0 \\ 0 & 0 & e^{-i\phi} \end{bmatrix}, \tag{21}$$

on the single-qutrit basis states, we vary the time-dependent qutrit frequency such that

$$\theta = \int_0^{t_{\rm phase}} \Delta(t)dt, \quad \phi = \int_0^{t_{\rm phase}} (2\Delta(t) - \eta)dt. \tag{22}$$

Equation (22) is satisfied if we set

$$t_{\rm phase} = \frac{2\theta - \phi}{\eta}, \quad \Delta_{\rm max} = \frac{\eta\theta}{2\theta - \phi - 2\eta}, \tag{23}$$

assuming a trapezoidal pulse for $\Delta(t)$ with a 2-ns ramp, and $\Delta_{\rm max}$ being the maximum value. Equation (23) can always be satisfied with a proper choice of θ and ϕ modulo 2π.

E. State-transfer fidelity

The state transfer considered in this section requires one qutrit to be in an arbitrary state $|\psi\rangle$, while the other qutrit is in the $|0\rangle$ state. The state-transfer operation $U_{\rm QST}$ can, therefore, be represented in matrix form in the basis

$$\{|00\rangle, |01\rangle, |10\rangle, |02\rangle, |20\rangle\} \tag{24}$$

as

$$U_{\rm QST} = \begin{bmatrix} 1 & 0 & 0 & 0 & 0 \\ 0 & 0 & 1 & 0 & 0 \\ 0 & 1 & 0 & 0 & 0 \\ 0 & 0 & 0 & 0 & 1 \\ 0 & 0 & 0 & 1 & 0 \end{bmatrix}. \tag{25}$$

If $U_{\rm obt}$ is the time-evolution operator obtained under the control pulse shown in Fig. 1(a), then the fidelity $\mathcal{F}$ between $U_{\rm obt}$ and $U_{\rm QST}$ is defined as [32]

$$\mathcal{F} = \frac{{\rm Tr}(\widehat{\mathcal{P}} U_{\rm obt} U_{\rm obt}^{\dagger} \widehat{\mathcal{P}}) + |{\rm Tr}(U_{\rm QST}^{\dagger} \widehat{\mathcal{P}} U_{\rm obt} \widehat{\mathcal{P}})|^2}{d(d+1)}, \tag{26}$$

where $\widehat{\mathcal{P}}$ is the projection operator that projects the time-evolution operator $U_{\rm obt}$ into the computational subspace (24), and d is the dimension of the computational subspace, which is 5 for this case. In the absence of decoherence, the dominant source of error in state transfer is the leakage to the $|11\rangle$ state in the double-excitation subspace [34], while the phase compensation operation is exact under the model considered for this work. We, therefore, can replace $U_{\rm obt}$ by $|U_{\rm obt}|$ in Eq. (26) and compute $\mathcal{F}$, which characterizes the fidelity for both the state transfer and the population transfer.

III. STATE TRANSFER ACROSS A CHAIN OF NEAREST-NEIGHBOR-COUPLED QUTRITS

Here I describe the model for an array of nearest-neighbor-coupled transmons and then discuss the QST across the chain of transmon quirts.

A. Array of coupled qutrits

Following the same technique as adopted in Sec. II A to derive the coupled-qutrit Hamiltonian (10), we can show that the Hamiltonian for a system of N nearest-neighbor-coupled superconducting qutrits is given by (from rotating frame)

$$\widetilde{H}_N(t) = \sum_{k=1}^{N} \begin{bmatrix} 0 & 0 & 0 \\ 0 & \Delta_{\rm k}(t) & 0 \\ 0 & 0 & 2\Delta_{\rm k}(t) - \eta \end{bmatrix}_{\rm q_k} + \sum_{k=1}^{N-1} \frac{g_k(t)}{2}(X_k X_{k+1} + Y_k Y_{k+1}), \tag{27}$$

where Δ_k is frequency of the kth transmon measured in reference to the frequency of the rotating frame, and X_k and Y_k are three-dimensional generalizations of Pauli's σ^x and σ^y matrices (corresponding to the kth qutrit), as defined in Equations (5) and (11), respectively. While both the frequencies and coupling strengths are time dependent for our system, in order to perform QST we keep all the qutrits in resonance, i.e., $\Delta_k = 0$, $\forall\, k \in \{1,2,\ldots,N\}$, and control the coupling strengths g_k with external control pulses.

Our QST protocol is composed of sequential state-transfer steps between adjacent qutrits, which means for N qutrits we need to perform $N-1$ sequential QST operations. It is therefore equivalent if we explore the accumulation of error for our protocol as a function of number of qutrits or as a function of number of concatenated state-transfer steps. I here adopt the latter and analyze the error mechanisms for our approach in the next section.

B. State transfer protocol

As mentioned earlier, all the qutrits are always in resonance during our QST protocol, while the coupling strengths are changed sequentially to transfer our initial state successively from one qutrit to another via neighboring qutrits. Figure 2 shows our sequential trapezoidal control pulses for a QST across a chain of four coupled qutrits, where we use the optimal parameters (shown in Table I) obtained numerically for the two-qutrit state transfer. A state transfer across a chain of N

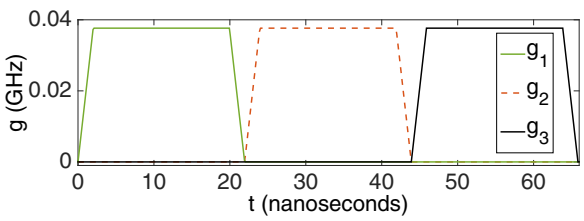

FIG. 2. (Color online) Trapezoidal pulses for $g_k(t)$ for a state transfer across a chain of four nearest-neighbor-coupled superconducting qutrits. To emulate a QST across a chain of N qutrits, we need to concatenate $(N-1)$ such pulses.

coupled qutrits requires concatenation of $(N-1)$ such pulses one after another, as mentioned earlier. I emphasize that it is sufficient for our QST protocol if we just optimize the pulse for a single qutrit-qutrit state transfer and then combine the pulses sequentially as shown in Fig. 2. This modularity is, in fact, required for any scalable QST protocols.

IV. ANALYSIS OF ERRORS

Here I discuss various error mechanisms relevant to our QST scheme. First, we estimate the errors generated from the unitary evolution under the control pulse (intrinsic errors), and then explore the effect of decoherence.

A. Intrinsic errors

Our QST scheme is composed of concatenating successive trapezoidal pulses for the coupling strengths, where the same set of optimal parameters is used for each pulse. Intrinsic errors are defined as errors originating from the unitary evolution of the system under the control pulse at $T_{1,2} \to \infty$ limit. To quantify how the intrinsic errors accumulate with sequential state-transfer steps, we prepare a uniform superposition $\psi_{\rm unif} = (|0\rangle + |1\rangle + |2\rangle)/\sqrt{3}$ in the first qutrit, and then compute the error after every state-transfer step to the adjacent qutrit. If ψ_k is the quantum state transferred at the kth step to the $(k+1)$th qutrit, then we define the intrinsic error as

$$\mathcal{E}_k^{\rm intr} = 1 - |\langle\psi_{\rm unif}|\psi_k\rangle|^2. \tag{28}$$

The blue (square) data points in Fig. 3 show the intrinsic error as a function of the number of steps, and we observe a quartic accumulation of intrinsic errors in that regime. The green (gray) curve in Fig. 3 is a quartic fit corresponding to $\mathcal{E}_k^{\rm intr} = \mathcal{A}k^4$, where the prefactor $\mathcal{A}$ is numerically determined to be $\sim 2.1 \times 10^{-10}$ for our case. The quartic accumulation of intrinsic errors, as opposed to an exponential accumulation [35], in fact allows us to perform a state transfer across a longer chain of superconducting qutrits.

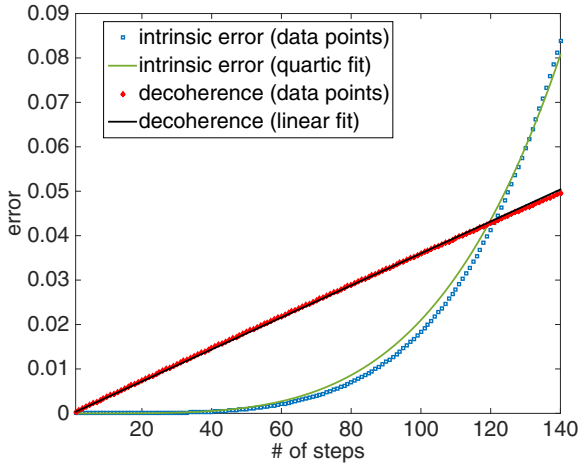

FIG. 3. (Color online) Accumulation of intrinsic and decoherence-induced errors with the number of steps. The red diamonds and blue squares are numerically computed data points, and the solid black and green (gray) curves are the linear and quartic fit for the decoherence-induced and intrinsic errors, respectively.

It should be emphasized at this point that many other error mechanisms can occur in a realistic setup, such as errors generated by the imperfect control electronics. Also, one can design different pulse shapes satisfying the constraint derived in this work, and imperfection in concatenating various pulse shapes can generate considerable intrinsic errors. While the robustness of my approach against such realistic noise mechanisms could be a topic of future research, I here consider a perfect experimental control and concatenation and analyze the intrinsic error that comes from the leakage of population into some undesired states.

B. Effects of decoherence

The model considered for this work assumes tunable couplings between adjacent qutrits, which means that during the entire state transfer, all the qutrits are decoupled from the system as well as remain in the ground state, except for the two neighboring qutrits participating in the QST. I therefore argue that the effects of decoherence on the qutrit state is essentially equivalent to that on a single qutrit prepared in the same state during the entire state-transfer process. To quantify the decoherence-induced errors on our QST scheme, we consider a single qutrit prepared in a uniform superposition $\psi_{\rm unif} = (|0\rangle + |1\rangle + |2\rangle)/\sqrt{3}$ (as considered for estimating the intrinsic errors), and construct the Kraus matrices for the amplitude and phase damping using the damped harmonic oscillator approximation [36]. We then perform the Kraus evolution for a time duration $kt_{\rm QST}$ (the time required for k successive state-transfer steps) on the single-qutrit density matrix ρ. The red (diamond-shaped) data points in Fig. 3 show the decoherence-induced error,

$$\mathcal{E}_k^{\rm decoh} = 1 - \langle\psi_{\rm unif}|\rho(kt_{\rm QST})|\psi_{\rm unif}\rangle, \tag{29}$$

as a function of k. The black line (almost aligned with the blue data points) in Fig. 3 shows the linear fit for the decoherence-induced error corresponding to $\mathcal{E}_k^{\rm decoh} = \mathcal{B}k$, where the prefactor $\mathcal{B}$ is numerically determined to be $\sim 3.6 \times 10^{-4}$. This numerical estimate of the slope of the linear fit in Fig. 3 is consistent with the approximate analytical estimate $t_{\rm QST}/T_{1,2}$ $(\approx 3.66 \times 10^{-4})$, where we assume $T_1 = T_2 = 60$ μs for the superconducting transmon qutrits [29]. It is interesting to note that for this case, decoherence is dominated by the intrinsic errors for $k > 120$, due the the quartic scaling of the intrinsic errors.

V. CONCLUSIONS

In this work, I have introduced a proposal for emulating a QST across a chain of spin-1 systems on a lattice of nearest-neighbor-coupled superconducting qutrits. While the emulation of higher spin systems with a single superconducting artificial atom has been demonstrated earlier [28], the problem transmitting a qutrit state along a chain of superconducting atoms has remained a nontrivial problem primarily due to the unequal coupling strengths in the single- and double-excitation subspaces. Here I have shown how to overcome this challenge with a proper choice of the control parameters under existing experimental conditions. My proposal thus motivates the simulation of various quantum transport processes

across higher spin systems, as well as enhanced quantum communication with scalable superconducting qutrits. Some possible future directions of this work include transmission of an arbitrary *qudit* state (a state encoded in a d-level quantum system) along a chain of coupled superconducting atoms and transfer of various entangled qutrit states across a chain of superconducting qutrits.

ACKNOWLEDGMENTS

I thank Barry Sanders for many illuminating comments as well as his careful reading of the manuscript. I also gratefully acknowledge useful discussions with David Feder, Michael Geller, and Pedram Roushan. This research was funded by NSERC, AITF and University of Calgary's Eyes High Fellowship Program.

[1] S. Bose, Phys. Rev. Lett. **91**, 207901 (2003).
[2] C. Albanese, M. Christandl, N. Datta, and A. Ekert, Phys. Rev. Lett. **93**, 230502 (2004).
[3] V. Subrahmanyam, Phys. Rev. A **69**, 034304 (2004).
[4] K. Korzekwa, P. Machnikowski, and P. Horodecki, Phys. Rev. A **89**, 062301 (2014).
[5] C. Di Franco, M. Paternostro, and M. S. Kim, Phys. Rev. Lett. **101**, 230502 (2008).
[6] S. Bose, Contemp. Phys. **48**, 13 (2007).
[7] A. Kay, Int. J. Quantum Inform. **08**, 641 (2010).
[8] P. Cappellaro, C. Ramanathan, and D. G. Cory, Phys. Rev. Lett. **99**, 250506 (2007).
[9] A. Ajoy, R. K. Rao, A. Kumar, and P. Rungta, Phys. Rev. A **85**, 030303 (2012).
[10] G. Kaur and P. Cappellaro, New J. Phys. **14**, 083005 (2012).
[11] M. Müller, L. Liang, I. Lesanovsky, and P. Zoller, New J. Phys. **10**, 093009 (2008).
[12] Y. Liu and D. Zhou, arXiv:1405.2634.
[13] A. Lyakhov and C. Bruder, New J. Phys. **7**, 181 (2005).
[14] K. R. K. Rao, T. S. Mahesh, and A. Kumar, Phys. Rev. A **90**, 012306 (2014).
[15] M. Bellec, G. M. Nikolopoulos, and S. Tzortzakis, Opt. Lett. **37**, 4504 (2012).
[16] A. Perez-Leija, R. Keil, A. Kay, H. Moya-Cessa, S. Nolte, L.-C. Kwek, B. M. Rodríguez-Lara, A. Szameit, and D. N. Christodoulides, Phys. Rev. A **87**, 012309 (2013).
[17] T. Fukuhara, A. Kantian, M. Endres, M. Cheneau, P. Schausz, S. Hild, D. Bellem, U. Schollwock, T. Giamarchi, C. Gross, I. Bloch, and S. Kuhr, Nat. Phys. **9**, 235 (2013).
[18] T. Fukuhara, P. Schausz, M. Endres, S. Hild, M. Cheneau, I. Bloch, and C. Gross, Nature **502**, 76 (2013).
[19] H. Bechmann-Pasquinucci and W. Tittel, Phys. Rev. A **61**, 062308 (2000).
[20] T. Durt, N. J. Cerf, N. Gisin, and M. Żukowski, Phys. Rev. A **67**, 012311 (2003).
[21] K. Eckert, O. Romero-Isart, and A. Sanpera, New J. Phys. **9**, 155 (2007).
[22] W. Qin, C. Wang, and G. L. Long, Phys. Rev. A **87**, 012339 (2013).
[23] M. Asoudeh and V. Karimipour, Quantum Inform. Process. **13**, 601 (2014).
[24] A. Bayat, Phys. Rev. A **89**, 062302 (2014).
[25] O. Romero-Isart, K. Eckert, and A. Sanpera, Phys. Rev. A **75**, 050303 (2007).
[26] M. Wiesniak, A. Dutta, and J. Ryu, arXiv:1312.6543.
[27] A. Delgado, C. Saavedra, and J. Retamal, Phys. Lett. A **370**, 22 (2007).
[28] M. Neeley, M. Ansmann, R. C. Bialczak, M. Hofheinz, E. Lucero, A. D. O'Connell, D. Sank, H. Wang, J. Wenner, A. N. Cleland, M. R. Geller, and J. M. Martinis, Science **325**, 722 (2009).
[29] R. Barends, J. Kelly, A. Megrant, A. Veitia, D. Sank, E. Jeffrey, T. C. White, J. Mutus, A. G. Fowler, B. Campbell, Y. Chen, Z. Chen, B. Chiaro, A. Dunsworth, C. Neill, P. O'Malley, P. Roushan, A. Vainsencher, J. Wenner, A. N. Korotkov, A. N. Cleland, and J. M. Martinis, Nature **508**, 500 (2014).
[30] Y. Chen, C. Neill, P. Roushan, N. Leung, M. Fang, R. Barends, J. Kelly, B. Campbell, Z. Chen, B. Chiaro, A. Dunsworth, E. Jeffrey, A. Megrant, J. Y. Mutus, P. J. J. O'Malley, C. M. Quintana, D. Sank, A. Vainsencher, J. Wenner, T. C. White, M. R. Geller, A. N. Cleland, and J. M. Martinis, Phys. Rev. Lett. **113**, 220502 (2014).
[31] M. R. Geller, E. Donate, Y. Chen, C. Neill, P. Roushan, and J. M. Martinis, arXiv:1405.1915.
[32] J. Ghosh, A. Galiautdinov, Z. Zhou, A. N. Korotkov, J. M. Martinis, and M. R. Geller, Phys. Rev. A **87**, 022309 (2013).
[33] One can construct an arbitrary pulse shape that satisfies Eq. (16). However, I here analyze a trapezoidal pulse because it is analytically tractable and it closely approximates a realistic pulse generated by the control electronics for superconducting circuits.
[34] J. Ghosh, A. G. Fowler, J. M. Martinis, and M. R. Geller, Phys. Rev. A **88**, 062329 (2013).
[35] R. Ronke, T. P. Spiller, and I. D'Amico, Phys. Rev. A **83**, 012325 (2011).
[36] Y.-x. Liu, S. K. Özdemir, A. Miranowicz, and N. Imoto, Phys. Rev. A **70**, 042308 (2004).